NASA TECHNICAL NOTE

NASA TN D-5067

NASA TN D-5067
c. 1

NASA TN D-5067

OPTICAL MODEL ANALYSIS OF PROTON SCATTERING IN THE RANGE 16 TO 22 MeV

by Edmund T. Boschitz

Lewis Research Center

Cleveland, Ohio

NATIONAL AERONAUTICS AND SPACE ADMINISTRATION • WASHINGTON, D. C. • APRIL 1969

OPTICAL MODEL ANALYSIS OF PROTON SCATTERING IN THE RANGE 16 TO 22 MeV

By Edmund T. Boschitz

Lewis Research Center
Cleveland, Ohio

NATIONAL AERONAUTICS AND SPACE ADMINISTRATION

For sale by the Clearinghouse for Federal Scientific and Technical Information
Springfield, Virginia 22151 – CFSTI price $3.00

ABSTRACT

Polarization, differential cross-section, and total reaction cross-section data for the scattering of 16- to 22-MeV protons from complex nuclei were analyzed with the optical model. An average potential was obtained which describes most of the data. Deviations from the average spin-orbit potential were observed for nuclei with doubly closed shells. The analysis of the energy dependence of proton scattering from O^{16} showed that a smooth variation of the optical model parameters results in satisfactory fits to the data between 30 and 50 MeV. The parameters cannot be extrapolated into the 20-MeV range.

OPTICAL MODEL ANALYSIS OF PROTON SCATTERING IN THE RANGE 16 TO 22 MeV

by Edmund T. Boschitz

Lewis Research Center

SUMMARY

An optical model analysis was performed of differential cross sections, polarizations, and total reaction cross sections for the scattering of protons from many nuclei in the energy region 16 to 22 MeV. An average potential consisting of nine parameters was obtained which predicts polarizations, differential cross sections, and reaction cross sections fairly well for most nuclei with masses larger than 30.

The parameters of the real central potential agree with those proposed earlier by Perey. The strength and width of the surface absorption potential increase with the target mass. Fits to the polarization data yield a spin-orbit potential with a radius and diffuseness smaller than those of the real central well. Anomalously low values for the parameters of the spin-orbit term were found in the mass regions of doubly closed shells. The effect is most pronounced for Ca^{40}. The analysis of the energy dependence of the proton scattering from O^{16} showed that it is impossible to extrapolate the smooth variation of the optical model parameters between 30 and 50 MeV to lower energies.

INTRODUCTION

It is an established fact that the elastic scattering of intermediate energy nucleons by heavier nuclei can be well described by the nuclear optical model. Most of the analyses, however, until recently, were based on differential cross-section data only, since polarizations and total reaction cross sections were rare. For this reason, the analyses gave little information about the spin-dependent part in the potential and left uncertainties in the imaginary part.

Systematic polarization studies were started by Rosen and Brolley (ref. 1) in 1958. Their extensive work between 8.0 and 14.5 MeV covered a wide range of nuclei. Unfor-

tunately, the polarization observed at these energies becomes quite small for nuclei in the upper half of the periodic table.

The elastic scattering of 18.5 and 20.5 MeV polarized protons by complex nuclei was studied extensively at this laboratory in past years (refs. 2 to 4). The experimental work was motivated by the need for more systematic polarization data at higher energies where sizable polarizations were expected for the heavy nuclei as well. In addition, the scattering by sets of isotopes and isobars should reveal the sensitivity of the polarization to the nuclear surface structure. This is quite plausible because the spin-orbit potential in its presently accepted form is proportional to the derivative of the central potential. Light nuclei were included in the polarization experiment in order to learn about the limitations of the optical model.

Parallel to this work, Baugh et al. (refs. 5 and 6) have investigated the polarization for 17.8-MeV protons scattered from a number of nuclei. The measurements extend only to a 120^{o} laboratory angle. This is unfortunate since the polarization distribution at large angles is quite significant for the analysis. The results of an optical analysis of data limited in angle might contain additional ambiguities.

More recently polarization data have become available at 30 and 50 MeV from the Rutherford Laboratory (refs. 7 to 10) and UCLA (private communication from W. T. H. van Oers), and at 40 MeV from the University of Minnesota (ref. 11) and the Oak Ridge National Laboratory (ref. 12).

In the present report, an optical model analysis is reported which uses polarization and differential cross-section data from this laboratory and also cross sections from the literature. In this study the emphasis is placed on the properties of the spin-orbit potential (i.e., its shape and its dependence on the bombarding energy and on the mass of the target nuclei).

SYMBOLS

A	nuclear mass number
a	diffuseness parameter of real central potential
a_I	diffuseness parameter of surface imaginary potential
a_{so}	diffuseness parameter of spin-orbit potential
c	velocity of light
E	proton energy
F	unit of length (10^{-13} cm)
$\hbar$	Planck's constant divided by 2π

$\vec{l}$	angular momentum vector
m_π	rest mass of π meson
P_{exp}	experimental polarization
ΔP_{exp}	estimated error in P_{exp}
P_{th}	theoretical polarization
r	radius of real central potential
r_c	radius of Coulomb potential
r_I	radius of imaginary potential
r_{so}	radius of spin-orbit potential
V	real central potential
V_c	Coulomb potential
V_{so}	spin-orbit potential
W	volume part of imaginary potential
W_D	surface part of imaginary potential
Z	nuclear charge number
Θ_{CM}	scattering angle in center of mass system
$\vec{\sigma}$	Pauli spin operator
σ_{exp}	experimental differential cross section
$\Delta\sigma_{exp}$	estimated error in σ_{exp}
σ_{th}	theoretical differential cross section
χ^2	measure of goodness of fit

PREVIOUS ANALYSES IN THE RANGE 16 TO 22 MeV

Two detailed optical model analyses exist in the literature in the energy range of the NASA data. Perey (ref. 13) has analyzed the differential cross sections for elastic protons scattering between 7 and 22 MeV with the emphasis on finding smooth trends in the parameters. His analysis resulted in an average potential which contains energy and mass dependences in a number of parameters. Rosen et al. (ref. 14) on the other hand, used the large amount of polarization data at 8.0, 10.5, and 14.5 MeV in addition to the existing cross-section data in order to establish a simple "universal" potential which

TABLE I. - COMPARISON OF "AVERAGE" POTENTIALS GIVEN BY PEREY (REF. 13) AND ROSEN ET AL. (REF. 14)

Parameter	Rosen	Perey
V, MeV	$53.8 - 0.33E$	$53.3 - 0.55E + 0.4\frac{Z}{A^{1/3}} + 27\frac{N-Z}{A}$
W, MeV	7.5	13.5±2 below $E_p = 17$; $3A^{1/3} \pm 1.5$ above
V_{so}, MeV	5.5	8.5 for $17 \leq E_p \leq 22$; 7.5 for $E_p < 17$
$a = a_{so}$, F	0.65	0.65
a_I, F	0.70	0.47
$r_o = r_I = r_{so}$, F	1.25	1.25

would describe the scattering of nucleons by nuclei over a wide range of energies and nuclear masses.

The two sets of parameters are listed in table I. The various terms are defined in the symbol list. The simplicity of Rosen's potential is quite appealing. In figure 1 predictions from both potentials are compared with the measured polarizations at 20.5 MeV. The solid lines correspond to Rosen's potential, and the dashed ones to Perey's parameters. Both potentials do poorly on the light nuclei. For the medium weight nuclei, Rosen's predictions are fairly good, but with increasing target mass the theoretical predictions become too large and get "out of phase." Similar difficulties are encountered in fitting the differential cross sections at 22.2 MeV. Perey's potential shows the opposite trend; it does poorly in the nickel region but improves for the heavier nuclei. The second fact can be attributed to the increase of the imaginary well depth with target mass.

In regard to predicting the total reaction cross sections (refs. 15 and 16), Rosen's potential produces a value which is 30 percent too large for nuclei up to mass 100; Perey's potential gives reaction cross sections which are too low for heavy nuclei (see fig. 6).

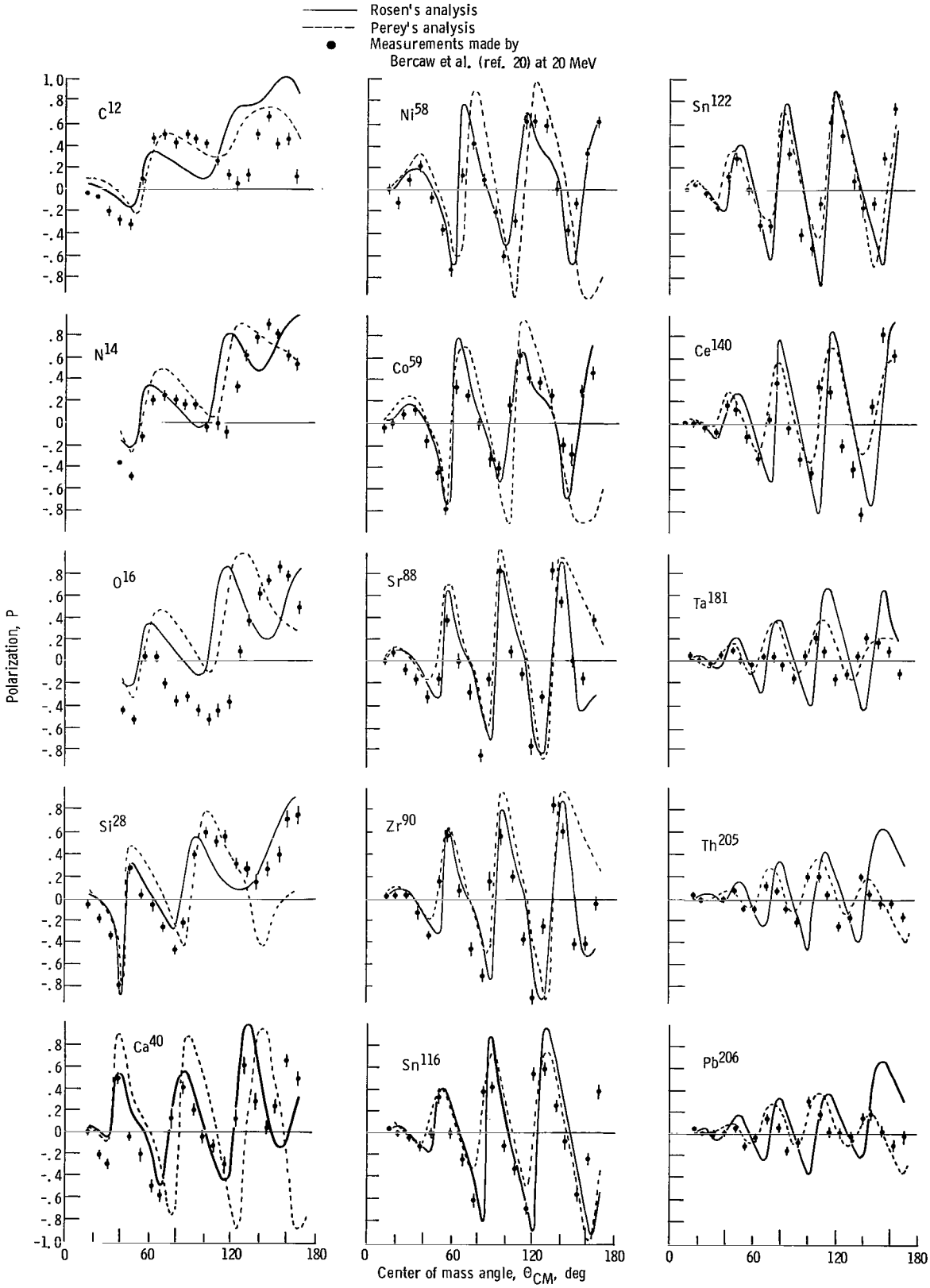

Figure 1. - Polarizations predicted by potentials of Rosen and Perey.

METHODS OF ANALYSIS

The present analysis was performed with a modified version of SCAT 4 (ref. 17) and Davidon's automatic search routine (ref. 18), which minimizes the quantities X_σ^2 and X_P^2 where

$$X_\sigma^2 = \sum_{i=1}^{n} \left[\frac{\sigma_{th}(\theta_i) - \sigma_{exp}(\theta_i)}{\Delta\sigma_{exp}(\theta_i)} \right]^2$$

$$X_P^2 = \sum_{i=1}^{n} \left[\frac{P_{th}(\theta_i) - P_{exp}(\theta_i)}{P_{exp}(\theta_i)} \right]^2$$

The calculation was performed on the IBM 7094 computer. Although the minimum X^2 was generally accepted as a criterion of best fit, visual inspection of goodness of fit served as an additional requirement. This becomes necessary when X_P^2 is large and a decrease in X_P^2 contradicts the shape of the polarization angular distribution. Also, an inferior fit from the X^2 point of view might be acceptable when the angular resolution typical for polarization measurements is considered. The optical potential used in this analysis is local and has the usual form

$$V(r) = V_c - V\left(\frac{1}{e^x + 1}\right) - i\left(W - 4 W_D \frac{d}{dx'}\right)\left(\frac{1}{e^{x'} + 1}\right) + \left(\frac{\hbar}{m_\pi c}\right)^2 V_{so} \frac{1}{r}\frac{d}{dr}\left(\frac{1}{e^{x_{so}} + 1}\right)\vec{\sigma} \cdot \vec{l}$$

where

$$x = \frac{r - r_o A^{1/3}}{a}$$

$$x' = \frac{r - r_I A^{1/3}}{a_I}$$

$$x_{so} = \frac{r - r_{so} A^{1/3}}{a_{so}}$$

and V_c is the Coulomb potential corresponding to a uniformly charged sphere of radius $r_c = 1.25\ A^{1/3}F$.

At the time when the polarizations were measured at this laboratory, it was assumed that later differential cross sections could also be measured for all nuclei at the same proton energy. Unfortunately - until now - matching cross sections became available only in a few cases. In most cases one had to be content with differential cross sections and total reaction cross sections at neighboring energies and in some cases even at neighboring nuclear masses. The following data were used:

(1) 40 polarization angular distributions (between 15^o and 165^o laboratory angles) of the energies 16.6, 18.5, and 20.5 MeV (Bercaw et al. (refs. 19 and 20))

(2) 25 differential cross sections at 17.0 (Dayton and Schrank (ref. 21)), 18.5 (Eccles et al. (ref. 22)), 20.5 (Gray et al. (refs. 23 to 25) and private communication from N. Baron, Lewis Research Center), and 22.2 MeV (Fulmer (ref. 26))

(3) 7 total reaction cross sections at 16.4 (Pollock and Schrank (ref. 15)) and 22.2 MeV (Fulmer (ref. 16))

The analysis of such unrelated sets of data required a special approach. The analysis was performed in two steps:

(1) In the first step an attempt was made to find an improved "average" potential (with constrained spin-orbit coupling, i.e., $a_{so} = a$ and $r_{so} = r_o$) which would give a "reasonable" fit to all data in this energy range. This was done in various ways. In faborable cases where polarizations and differential cross sections existed at the same energy, the sum $X_T^2 = X_\sigma^2 + X_P^2$ was minimized directly. In other cases where both kinds of data were available only at different energies, either $X_T^2 = X_\sigma^2 + X_P^2$ was minimized for the average energy or X_σ^2 and X_P^2 were minimized separately (each at the correct energy); then the "optimum" parameter pairs were gradually adjusted to converge to one value which produced a compromise fit to both kinds of data. In the majority of the cases, the best method appeared to be the minimizing of X_σ^2 and X_P^2 for all nuclei and energies individually for a given search on two or three parameters. The widely fluctuating parameters which resulted from this search were then plotted against nuclear mass and bombarding energy and common trends were investigated. These trends were used in the next search on different parameters and new smooth trends were established. This method seems appropriate since one is looking for "average" trends in the true spirit of the optical model. There are much less data available for the total reaction cross sections. Therefore, they were not included in the search, but they served as a guide to reject parameter values which did not predict the reaction cross sections correctly.

(2) In the second step, the trends of the spin-orbit potential were to be investigated. In order to see those trends, the fluctuations of the other parameters must be averaged out. This was done by using the average central potential from step (1); now the search routine varied V_{so}, a_{so}, and r_{so}, minimizing X_P^2 only. An analysis under such "restricted conditions" is considered permissible since it is essentially the polarization which defines the parameter space of the spin-orbit potential. This assumption has been confirmed at low energy by Goldfarb et al. (ref. 27). They have shown that small deviations in the spin-orbit parameters could be treated as perturbations which affect the polarization but hardly change the cross section.

SEARCH FOR AVERAGE POTENTIAL

Central Potential (Constrained Spin-Orbit Potential)

The search was started from Rosen's potential since it is based on the analysis of both cross-section and polarization data. Also the simplicity of this potential is appealing. With the geometrical parameters kept fixed at first, combined searching and rough gridding on the depths of the potentials V, W_D, and V_{so} (W was set equal to zero) showed the following trends: All searches on W_D clearly indicate the need for an increase with nuclear mass. This mass dependence reduces the magnitude of the polarization for heavy nuclei, which is the main drawback of Rosen's parameter set, but it does not allow for the difference in the "phase" between theoretical and experimental polarization distributions. This difference can be removed only by a mass dependence in the real central well. Studying the mass (and energy) dependence of V in detail revealed that both dependences were reasonably close to the ones given by Perey (ref. 13). Therefore, from that point on the real potential V was set equal to V_{Perey}. Searches on $V_{so}(a_{so} = a,\ r_{so} = r_o)$ confirmed Rosen's value of 5.5 MeV. Now V, V_{so}, $a = a_{so}$, $r_o = r_{so}$ were kept fixed, and the imaginary potential was inspected more closely. In this part of the analysis, the total reaction cross section served as "a guide" to exclude sets of parameters which would give good fits to polarization and differential cross section, but which would not agree with the total reaction cross sections. In order to obtain the correct mass dependence of the imaginary well, the radius parameter r_I was varied in steps of 0.05 F between 1.15 and 1.35 F. For each value of r_I, the diffuseness a_I was varied in steps of 0.05 F between 0.45 and 0.75 F. For these various combinations, the computer code searched on W_D. The parameters $r_I = 1.25$ F, $a_I = 0.65$, and $W_D = 2A^{1/3}$ were found as an optimum set. Yet, the prediction of the reaction cross sections still needed improving. In reference 28 it is suggested that a_I might be larger for heavy nuclei, so various mass dependences were tried for a_I;

$a_I = 0.54 + (A/1000)$, $a_I = 0.45 + (A/250)$, $a_I = 0.38 + (A/550)$, and $a_I = 0.45 + (A/650)$ were chosen. The last mass dependence is most successful, and the corresponding values for W_D indicated that $W = 1.5A^{1/3} + 2.5$. The inclusions of a volume absorption W had little effect on the reaction cross section; it increases only by about 1 percent per 1 MeV well depth. In presenting average parameters for the imaginary potential, it should be pointed out that there are large fluctuations in W_D, as shown in figure 2. These fluctuations are probably due to the fact that W_D contains the "individualism" of the nucleus in regard to nuclear reactions and modes of excitation.

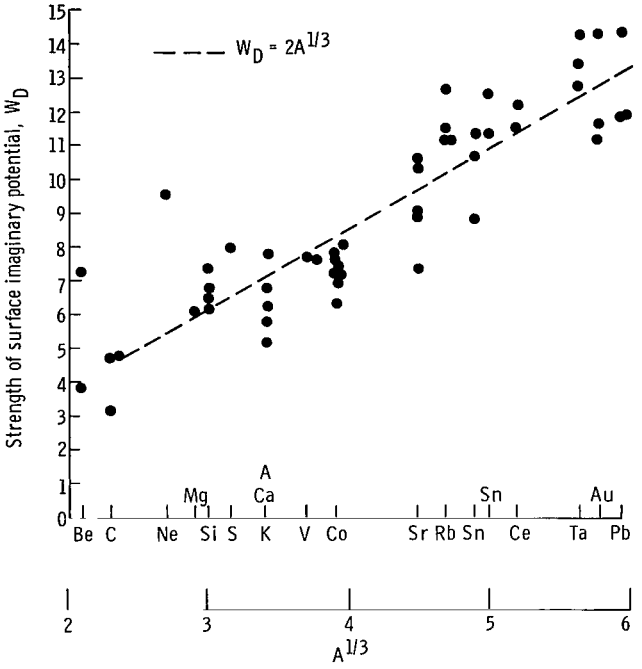

Figure 2. - Optimum values of W_D obtained from searching on W_D with remaining parameters fixed. ($a_I = 0.65$ F.)

Independent Spin-Orbit Potential (Fixed Central Potential)

After an average central potential was found, V, a, r_o, W_D, a_I, and r_I were fixed and the search code varied the parameters of the spin-orbit part, minimizing X_P^2 only. The optimum values from this "restricted" analysis were checked in eight cases where matching cross-section data were available. In these cases the search code varied V and W in addition to V_{so}, a_{so}, and r_{so}, which now minimized the sum $X_T^2 = X_P^2 + X_\sigma^2$. The optimum values for the spin-orbit potential parameters found by this "unrestricted" search differed only insignificantly from those obtained under the restricted condition,

verifying the validity of the method. The values for V_{so}, a_{so}, and r_{so} which correspond to the smallest X_P^2 are plotted as a function of nuclear mass in figure 3. This plot contains the results of the analyses of both 18.5- and 20.5-MeV data, since no energy dependence of the average parameters was apparent. With the exception of the light nuclei, the average trend of the parameters is indicated by the horizontal lines with the range of scatter given by the crosshatching. The average values are V_{so} = 5.5±0.5 MeV, a_{so} = 0.55±0.05 F, and r_{so} = 1.12±0.05 F.

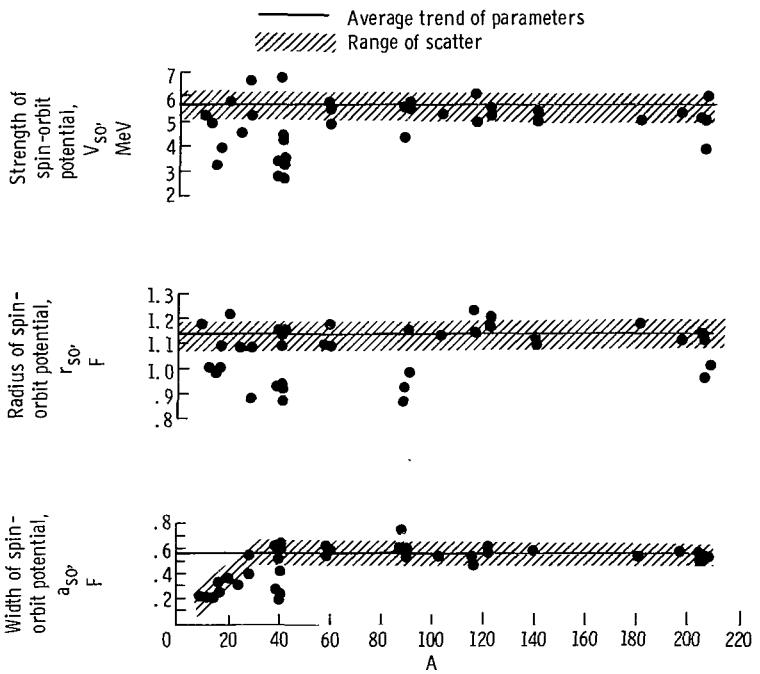

Figure 3. - Optimum values of V_{so}, a_{so}, and r_{so} obtained from searches on these parameters with parameters of central potential fixed. ($V = V_{Perey}$, $W = 2A^{1/3}$, $a = a_I = 0.65$ F, and $r = r_I = 1.25$ F.)

These average values together with the average parameters for the central potential ($V = V_{Perey}$, $a = 0.65$ F, $r = 1.25$ F, $W_D = 1.5\,A^{1/3} + 2.5$, $a_I = 0.45 + (A/650)$, and $r_I = 1.25$ F) produce the theoretical curves in figures 4 to 6. The overall agreement with the experimental data is quite good. The individual fits can certainly be improved if the well depths V, W_D, and V_{so} can vary freely. For a quantitative comparison, the paremeter sets of Rosen and Perey are listed in table II together with the average parameters from this analysis. Considering recent polarization data, Perey modified his first potential (ref. 29). The revised parameters are listed in column 4. In columns

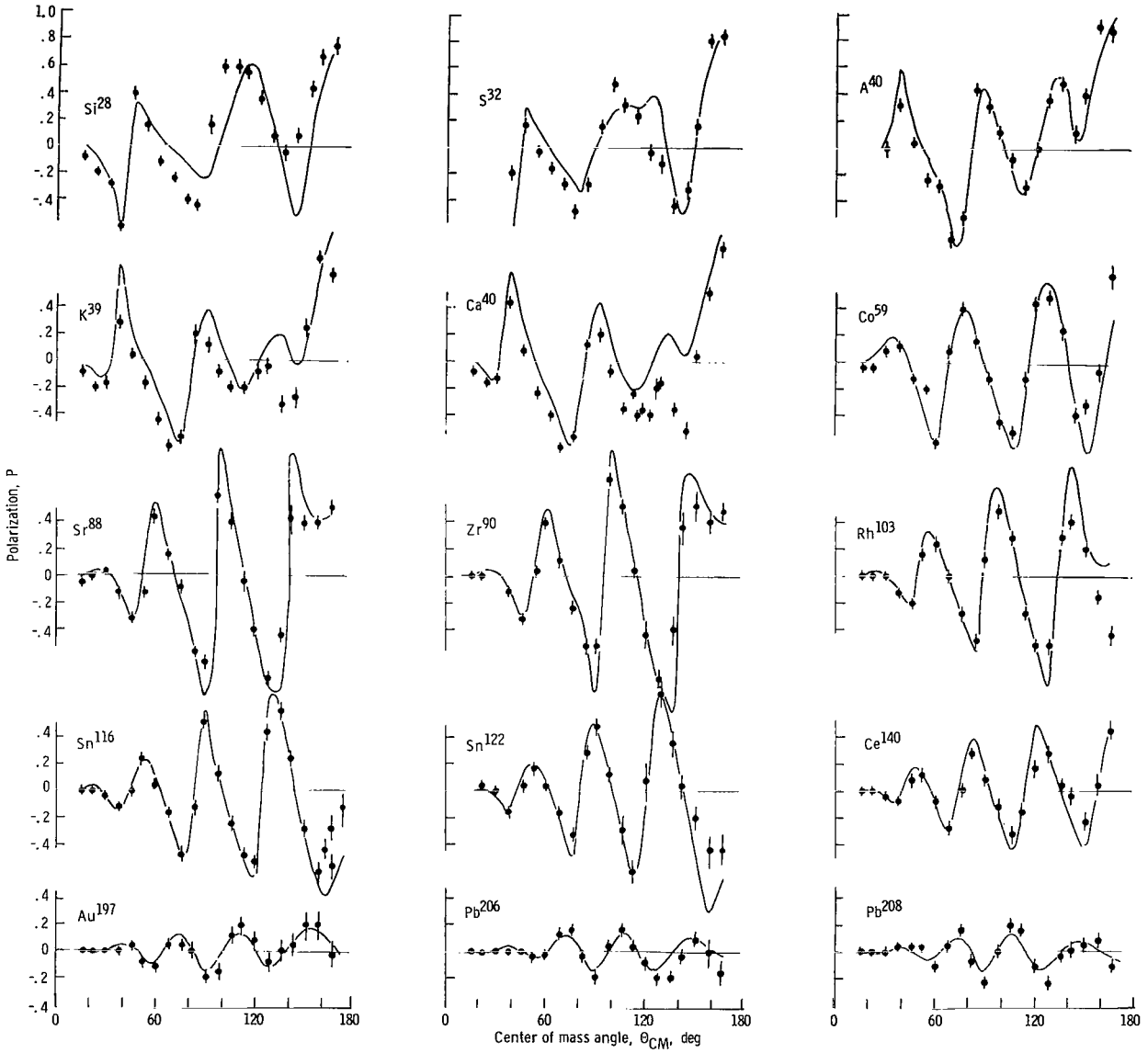

(a) Proton energy E_p = 18.5 MeV.

Figure 4. - Polarizations predicted by "average" potential listed in table II, column 6. (Data are from refs. 2 and 20.)

5 and 6 the results from this analysis are presented. The set in column 5 produces good fits to the polarizations and differential cross sections but is inferior in predicting the total reaction cross sections. The set in column 6 corrects for this. The comparison shows fairly good agreement with Perey's analysis, the difference being in W_D, a_I, V_{so}, and a_{so}. The mass dependence of V, W_D, and a_I are essential features of the optical model. Neglecting this dependence in Rosen's potential causes inferior fits to the data.

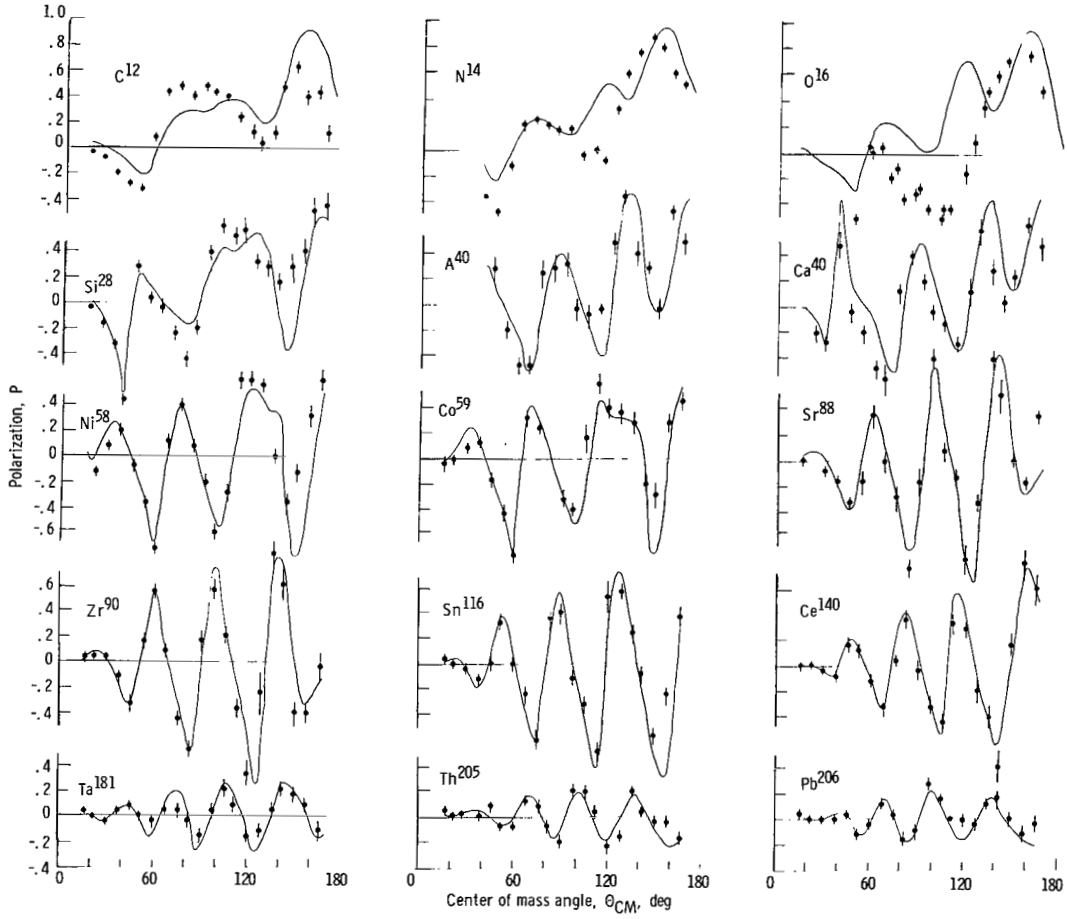

(b) Proton energy E_p = 20.5 MeV.

Figure 4. - Concluded.

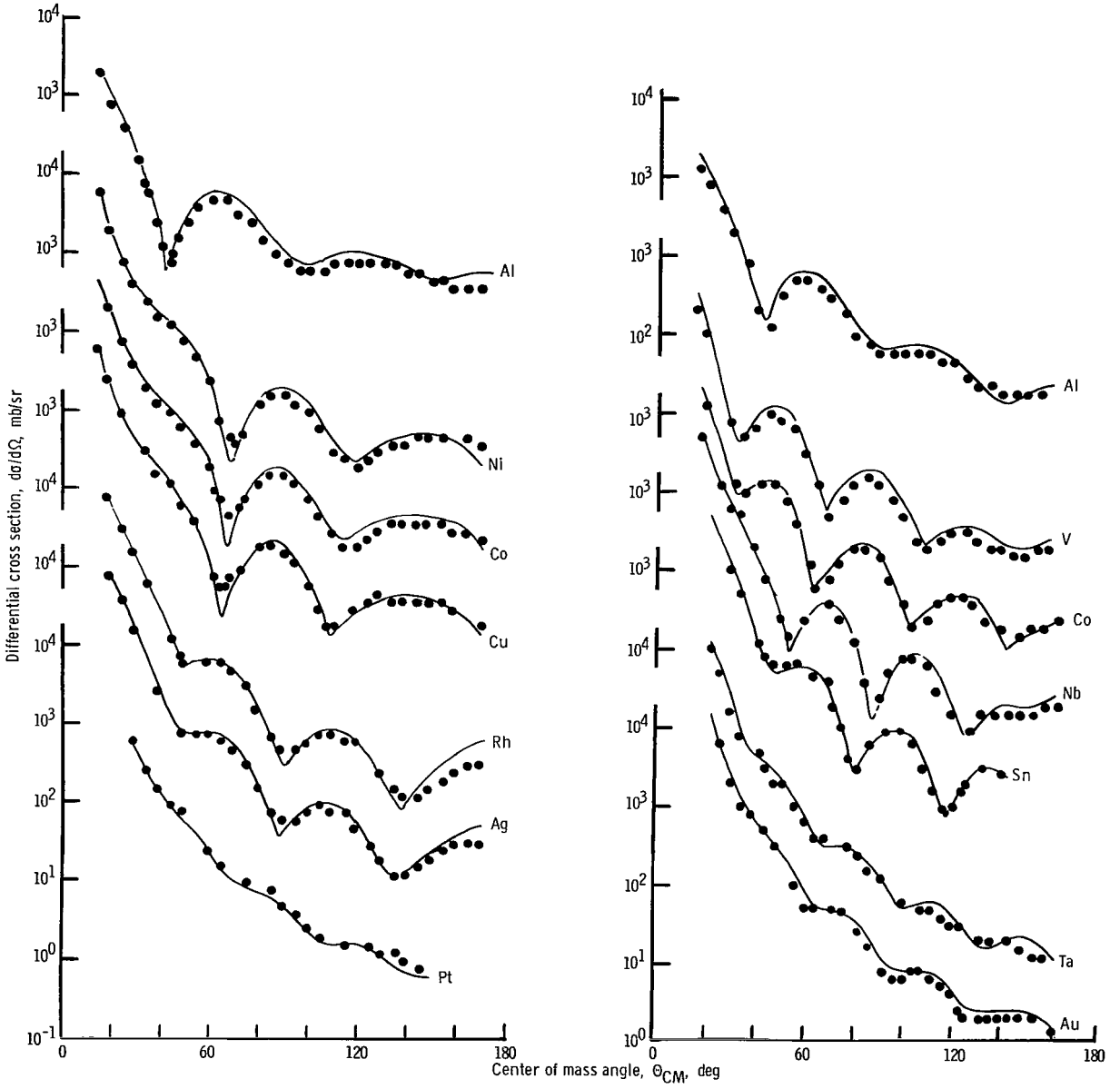

(a) Energy, 17 MeV. (Data from ref. 21.)

(b) Energy, 22.2 MeV. (Data from ref. 22.)

Figure 5. - Differential cross sections predicted by "average" potential listed in table II, column 6. (Data from refs. 21 and 22.)

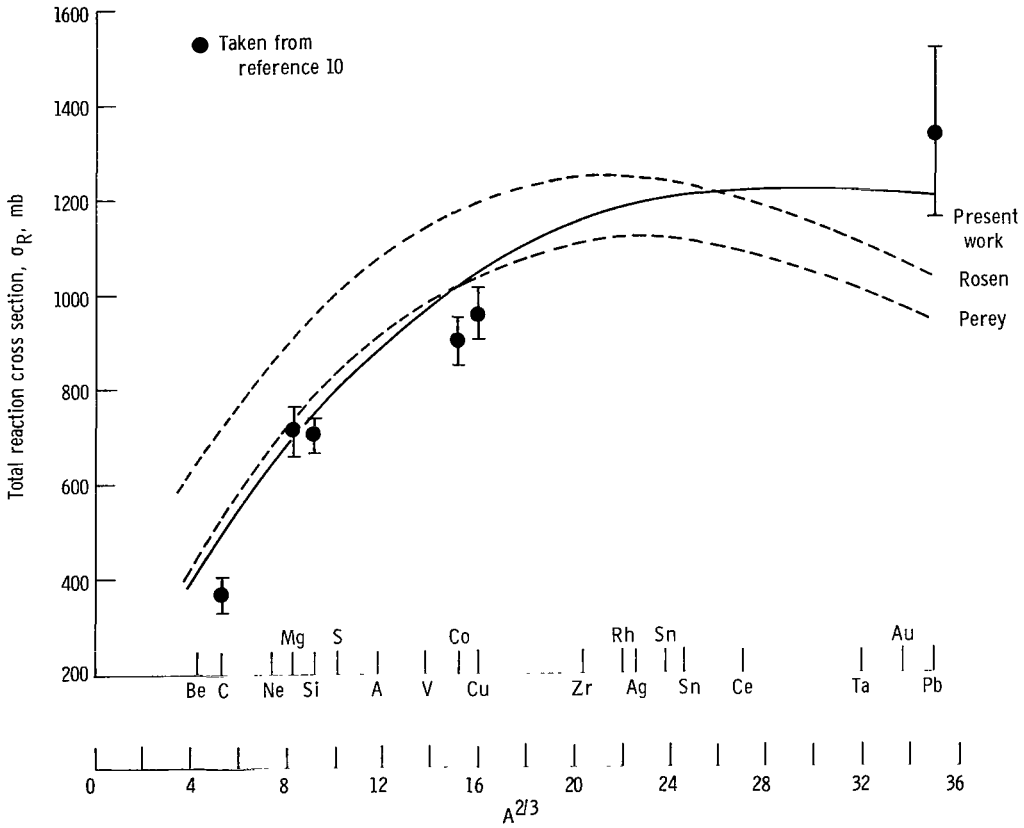

Figure 6. - Total reaction cross section predicted by "average" potential listed in table II, column 6.

TABLE II. - COMPARISON OF PREVIOUS POTENTIALS WITH BEST "AVERAGE" POTENTIALS FOUND IN THIS ANALYSIS

Parameter	Rosen	Perey		Present work	
		First	Second	First	Second
V, MeV	$53.8 - 0.33E$	$53.3 - 0.55E + 0.4\frac{Z}{A^{1/3}} + 27\frac{N-Z}{A}$	V_P	V_P	V_P
W_D, MeV	7.5	$3A^{1/3}$	$3A^{1/3}$	$2A^{1/3}$	$1.5A^{1/3} + 2.5$
V_{so}, MeV	5.5	8.5	6.0	5.5	5.5
a, F	0.65	0.65	0.65	0.65	0.65
a_{so}, F	0.65	0.65	0.47	0.55	0.55
a_I, F	0.70	0.47	0.47	0.65	$0.45 + \frac{A}{650}$
r_o, F	1.25	1.25	1.25	1.25	1.25
r_I, F	1.25	1.25	1.25	1.25	1.25
r_{so}, F	1.25	1.25	1.12	1.12	1.12
X^2_σ (^{a}17.0)	^{a}9.5	6.4	10.2	6.1	8.0
X^2_P (^{a}18.5)	27.0	49.0	15.5	11.6	11.8
X^2_σ (^{a}22.2)	20.4	16.7	19.4	6.3	6.4
X^2_P (^{a}20.5)	29.3	32.0	14.8	5.7	6.5
X^2_{av}	21.5	26.0	15.0	7.4	8.1

^{a}Values for X^2 are number of X^2's per data point.

ANOMALIES IN THE SPIN-ORBIT POTENTIAL (THE NUCLEI K^{39}, Ar^{40}, AND Ca^{40})

In figure 3 the average trend of the parameters V_{so}, a_{so}, and r_{so} is shown. There are deviations from the average values for the light nuclei ($A < 30$) which are discussed later. There are other mass regions, however, where considerable deviations from the average values occur. Anomalously low values are found around $A = 40$ (K^{39}, Ar^{40}, and Ca^{40}), $A = 90$ (Sr^{88} and Zr^{90}), and $A = 208$ (Pb^{206} and Pb^{208}) which

seem to be related to shell closure. The effect is most pronounced in the $A = 40$ region and less so in the other regions. The anomalous parameters show no regularities. For one nucleus, only r_{so} shows irregularity; for another, V_{so} and/or a_{so}; sometimes all three parameters have to be decreased to obtain good fits. This could be due to some ambiguities between V_{so}, a_{so}, and r_{so} similar to the well-known ones between V and r and W_D and a_I. If some ambiguities between the parameters of the spin-orbit potential do exist, then it might be possible to keep one or two parameters fixed and to assign the anomalous behavior to the remaining parameters. This was tried, but generally it was impossible to attribute the anomalies to just one or two of the three parameters. Some progress, however, was made in the $A = 40$ region, which is described in the following section.

Ca^{40} has been an interesting nucleus for quite a while. In the contest of the optical model, it is interesting because of the difficulties encountered in fitting the experimental data. In the course of the experiments at this laboratory, large differences in the polarization distributions were observed in the scattering of 18.5-MeV protons by Ar^{40}, K^{39}, and Ca^{40} (ref. 30).

Volkin performed an optical model analysis (ref. 31) of these data in order to explain these differences. He found that best fits were obtained by decreasing the radius parameter r_{so} from 1.25 to 1.18 F and 1.03 F when proceeding from Ar^{40} to K^{39} and Ca^{40}. He concluded that this decrease might be indicative of a shell closure effect in the nuclear optical model which appears in the form of the spin-orbit potential. For closed shell nuclei, the spin-orbit potential is centered approximately at the nuclear matter radius rather than at the central potential radius. Volkin also considered a complex spin-orbit potential to fit the data, but he concluded that there is no need for an imaginary part in the spin-orbit potential if a smaller radius ($r_{so} < r_o$) is used.

Baugh et al. (ref. 32) analyzed their p-Ca^{40} polarization angular distribution at 17.5 MeV with an imaginary part $W_{so} = 2$ MeV. To elaborate on this result, they measured the energy dependence of the polarization for this nucleus between 14.0 and 18.5 MeV (at four laboratory angles between 85^o and 115^o) and confirmed the earlier conclusion that $W_{so} \approx 2$ MeV over this energy range.

In the present work, the polarizations and differential cross sections for K^{39}, A^{40}, and Ca^{40} were analyzed in the energy range 14.5 to 21 MeV. At first, only V_{so}, a_{so}, and r_{so} were varied in combined rough gridding and searching; X_P^2 was thus minimized. It was found, as mentioned previously, that all three parameters tend to have smaller values than the average ones; but, if somewhat inferior fits (~30 percent increase in X^2) are accepted, $r_{so} = 1.1$ F can be kept fixed. In the following searches, $X_T^2 = X_P^2 + X_\sigma^2$ was minimized when V, W, V_{so}, and a_{so} were varied (where $a = a_I = 0.65$ F, $r_o = r_I = 1.25$ F, and $r_{so} = 1.1$ F). Both V and W were included in the search because differential cross-section data were used in this part of the analysis. The results are shown in figure 7; the corresponding parameters are listed in table III. A number of

interesting features should be pointed out. First, the depth of the real central well is smaller for Ar^{40} than for Ca^{40} contrary to the predictions from the asymmetry term in Perey's potential, where $V_{Ar^{40}} > V_{Ca^{40}}$ by 2.7 MeV. No explanation is found for this result. Second, the depths of the imaginary central well decrease monotonically with progressive shell closure, Ar^{40} K^{39} Ca^{40}. This might indicate that fewer inelastic channels are open for the closed shell nucleus. Third, the depths and widths of the spin-orbit potential, V_{so} and a_{so}, individually do not show a systematic behavior, but their product $V_{so}a_{so}$ does. This quantity might be interpreted as the "effective strength" of the spin-orbit coupling. The energy dependence of this "effective strength" is plotted in figure 8. The crosshatched area marks the range of scatter of the average parameters. The interesting features of this energy dependence are the systematically lower values of $V_{so}a_{so}$ for Ca^{40} at all energies and the occurrence of a minimum in the spin-orbit force for both Ar^{40} and Ca^{40} near 17 MeV. Both features might be understood qualitatively. The lower values of $V_{so}a_{so}$ for the Ca^{40} nucleus can probably be explained in terms of the spin-dependent part of the nucleon-nucleon potential. The nucleon-nucleon potential contains a tensor term (of longer range) and a spin-orbit term

TABLE III. - OPTIMUM PARAMETERS FOR Ar^{40}, K^{39}, AND Ca^{40} OBTAINED FROM SEARCHES ON V, W_D, V_{so}, AND a_{so} WITH THE USE OF POLARIZATION AND CROSS-SECTION DATA

[Geometric parameters: $a = a_I = 0.65$ F, $r_o = r_I = 1.25$ F, and $r_{so} = 1.10$ F.]

Energy, E, MeV	Nuclei	Depth of real potential, V	Depth of volume part of imaginary, W	Depth of spin-orbit potential, V_{so}	Width of spin-orbit potential, a_{so}	Effective strength, $V_{so}a_{so}$	Goodness of fit, χ^2_T
14.5	Ar	47.4	7.2	5.5	0.55	3.0	159
	Ca	48.4	5.2	5.0	.37	1.9	412
17.0	Ar	46.7	7.7	3.7	0.43	1.6	550
	Ca	47.9	5.2	4.2	.25	1.0	361
18.3	Ar	47.4	8.5	4.4	0.60	2.6	357
	K	48.7	6.4	4.0	.49	1.9	744
	Ca	48.0	5.4	3.8	.34	1.3	724
21.0	Ar	43.5	7.7	4.8	0.60	2.9	275
	K	[a]47.1	[a]8.4	4.5	.57	2.6	340
	Ca	[a]46.2	[a]8.2	4.6	.53	2.4	249

[a]Obtained from searches that used cross sections of neighboring nuclei.

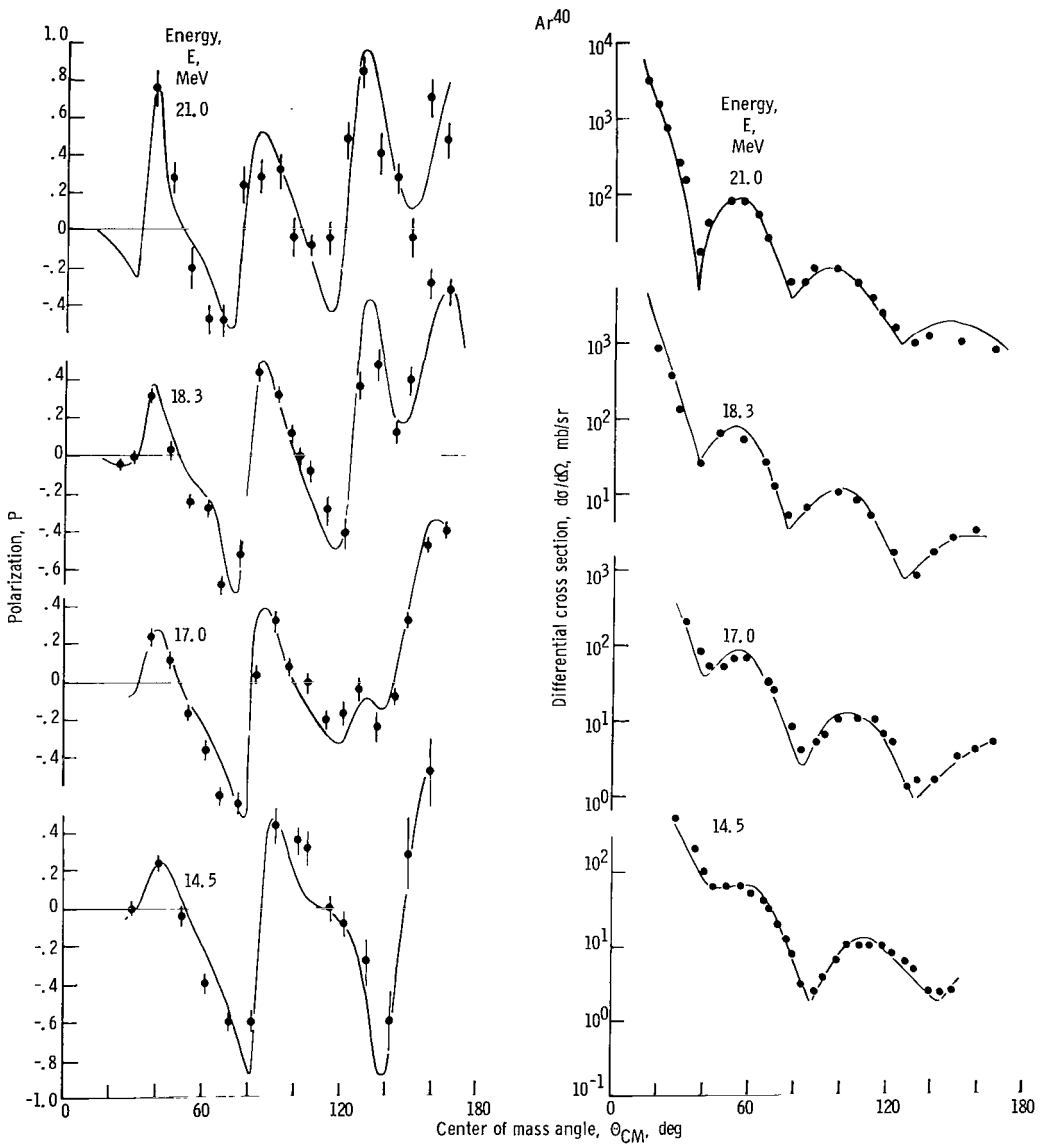

Figure 7. - Comparison of calculated polarizations and differential cross sections (parameters of table III) with experimental data of references 2, 20, 23 to 26, and private communication from N. Baron.

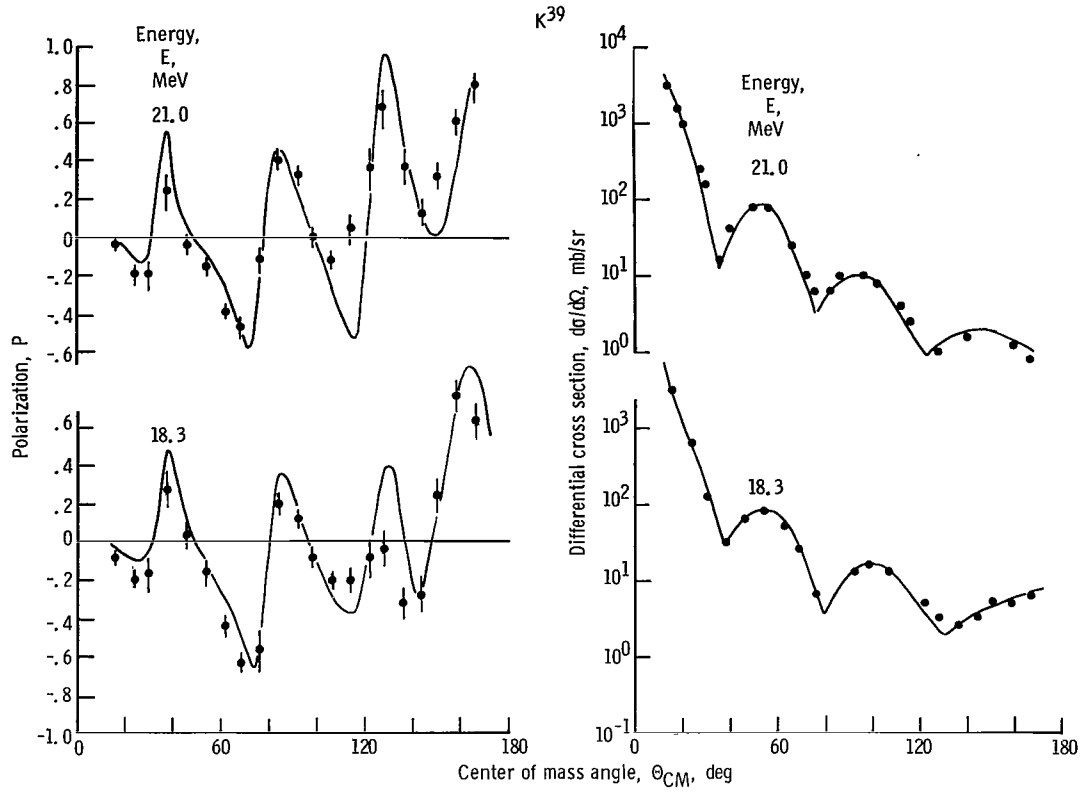

(b) K^{39}.

Figure 7. - Continued.

(of shorter range). For the doubly closed shell nucleus Ca^{40}, the tensor term will vanish, and the remaining (short range) nucleon-nucleon LS-term is responsible for the smaller parameter values in the spin-orbit term of the optical potential. The occurrence of a minimum in the "effective strength" near 17 MeV might be correlated with the entering of a new partial wave. In the scattering of 14.5-MeV protons from complex nuclei, Rosen and Stewart (ref. 33) have observed that in mass regions where $p \cdot R = n\hbar$ (corresponding to the entering of a new partial wave), the back angle polarization patterns are extremely sensitive to the addition of even a single nucleon in the target nucleus. The present analysis of A^{40}, K^{39}, and Ca^{40} indicates a similar sensitivity of the polarization. The question arises if a decrease in the spin-orbit force for Ca^{40} would also appear at the entering of the next partial wave at 30 MeV ($p \cdot R = 5\hbar$). Recently, polarization and cross-section data at 30 MeV (Rutherford Lab.) and at 40 MeV (Oak Ridge National Lab.) have been analyzed by Satchler (ref. 34) and Blumberg et al. (ref. 35). For Ca^{40} considerable difficulties were encountered in obtaining satisfactory fits to polarizations and cross sections simultaneously. However, the best fits obtained at 30 MeV required reduced values of V_{so} and a_{so}, resulting in a product of about 1 (MeV) (F), which is comparable to the findings at 17 MeV. At 40 MeV, no such effects are seen.

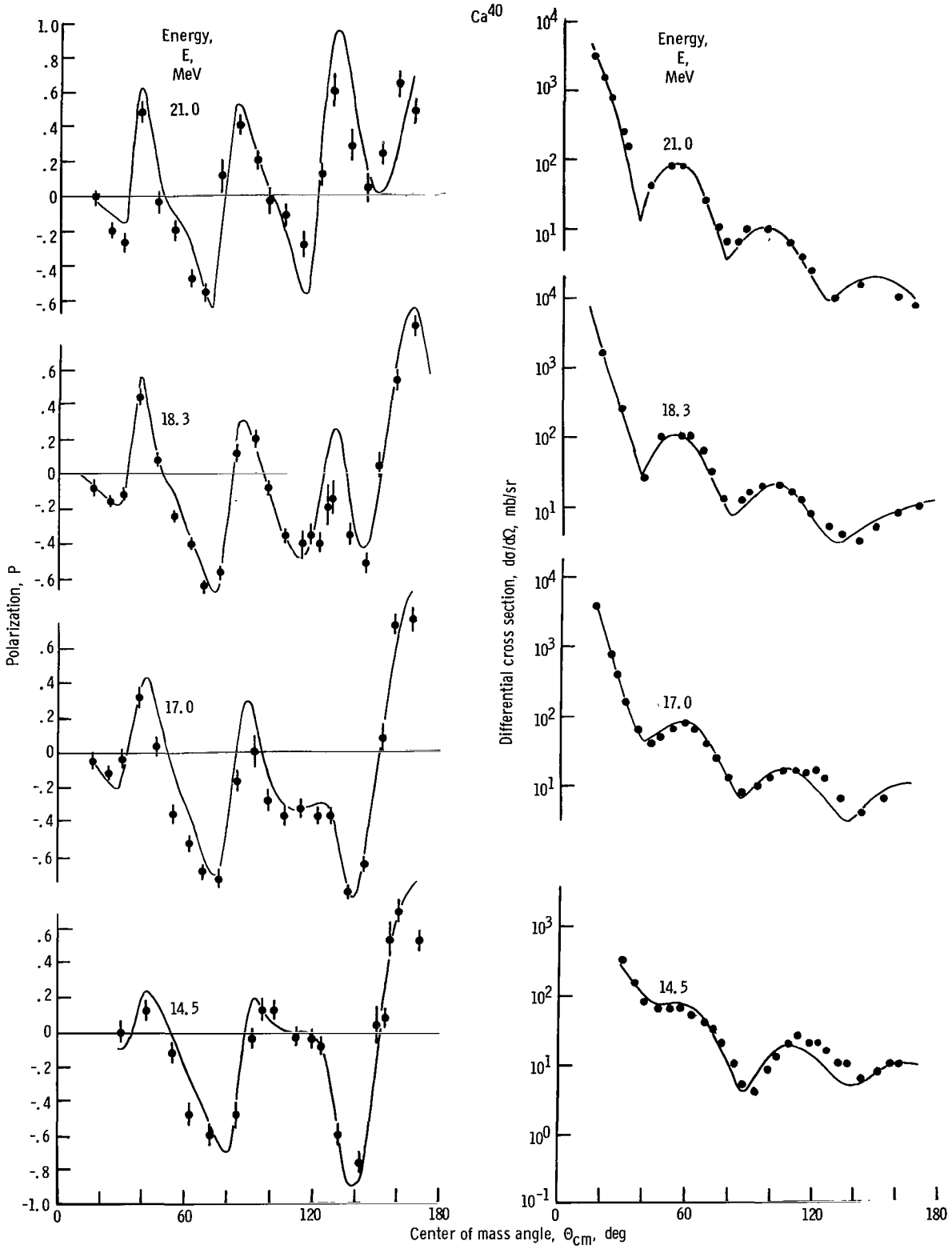

(c) Ca^{40}

Figure 7. - Concluded.

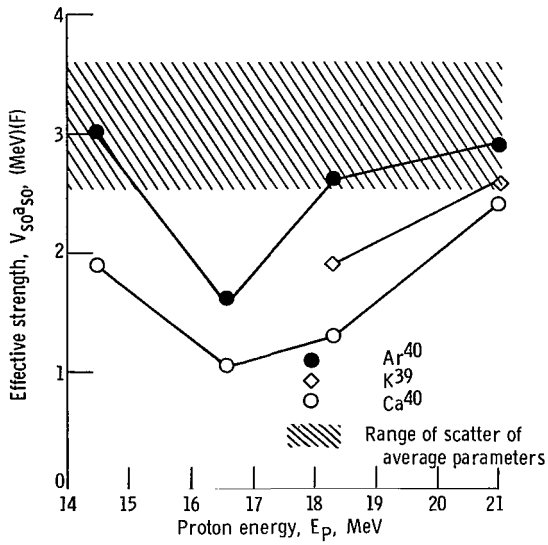

Figure 8. - "Effective strength" ($V_{so}a_{so}$) of spin-orbit coupling as function of bombarding energy.

LIGHT NUCLEI (ENERGY DEPENDENCE OF p-O^{16})

It has been shown that the average optical model potential (columns 4 and 5 of table II, p. 15) can describe differential cross sections, polarizations, and total reaction cross sections for the heavier nuclei very well. From figure 4 (p. 11) it is clear, however, that this is not true for the light nuclei ($A \lesssim 30$). In some cases (C^{12} at 20.5 MeV and Si^{28} and S^{32} at 18.5 MeV), there may be a qualitative agreement between theory and experiment; however, in other cases (N^{14} and O^{16}), there is complete failure. If the optical model parameters are allowed to vary freely, good fits can generally be obtained, but the parameters vary rapidly with energy and from one nucleus to the other. There are certain trends in some of the parameters, as can be seen in figure 3 (p. 10). The parameters of the spin-orbit coupling, in particular, the diffuseness a_{so}, tend to smaller values, but the meaning of this is not clear. Other analysis in this energy range also shows the rapid variation of the individual parameters. Differential cross sections have been analyzed for the p-C^{12} and p-O^{16} system between 10 and 20 MeV (refs. 36 and 37). Cross-section and polarization data have been used in the analysis of p-N^{14} scattering at 20.7 MeV (ref. 38) and p-O^{16} scattering at 16.3, 18.5, and 21.0 MeV (refs. 31 and 38).

The rapid variation of the parameters may be due to the existence of intermediate structures which can yield broad resonances (a few hundred keV wide) in the cross section. Lowe and Watson (ref. 39) have taken these resonances into account by adding a contribution due to the coupling of three states in N^{13} to the optical model scattering amplitudes. Between 20 and 30 MeV, p-C^{12} cross sections and polarizations have been

analyzed by Tamura and Teresawa (ref. 40). The nonmonotonic variations of the cross section with energy could be reasonably well explained by the optical model if Breit-Wigner resonance terms were added. However, neither the polarizations nor the reaction cross sections are well represented by the parameters from the analysis of Tamura and Teresawa.

For any further analysis of proton scattering by light nuclei in this "resonance region," it might be helpful to know how the optical potential would look if there were no resonances.

An optical model analysis of the type described previously (covering a large range in nuclear masses) is one way to proceed. The "average" parameters of the optical potential can be extrapolated into the region of low nuclear mass.

The other possibility is an optical model analysis for a typical light nucleus over a large energy range. If at high enough energies a region can be found where the optical model is valid, those "average" parameters might be extrapolated to lower energies. With the exception of C^{12} (which is a poor representative for light nuclei because of the strong coupling of the first excited state to the ground state), such a systematic study has not been done previously.

For this reason Boschitz et al. (ref. 41) have extended the p-O^{16} polarization measurements at NASA (at 16.3, 17.8, and 21.0 MeV) to 52.5 MeV, using the 88-inch cyclotron at Berkeley. The polarization data have been supplemented by differential cross-section measurements at 42.0 and 52.5 MeV. The polarization data are shown in figure 9. The lines drawn through the data points serve only to guide the eye. A significant change in the polarization pattern is found between 21 and 25 MeV. Above this energy, the polarization distributions vary slowly with energy. The analysis of these data has been performed in the following way:

First, only those data were considered for which there appears to be a smooth energy dependence. The search was limited to seven parameters, which meant setting the geometrical parameters of the spin-orbit term equal to the corresponding parameters of the central potential. The radius of the real central potential was successively fixed at 1.20, 1.25, and 1.30 F; the search code varied V, W, and V_{so}, while simultaneously gridding on a, a_I, and r_I. For the search at 32.8 MeV, the 30.3-MeV cross-section data from Harwell were used; while at 36.7 MeV, interpolated cross sections were used in the search routine. The best fits were selected by visual inspection under the constraint that the parameters were reasonable and compromising over the energy range. The best fits are seen in figure 10, and the corresponding parameters are tabulated in table IV. Clearly the agreement with the experimental data is not satisfactory, in particular, because all seven parameters are variables with energy.

For this reason, radius r_{so} and diffuseness a_{so} of the spin-orbit potential and volume absorption W were added to the variables to be searched. The greatest improvement in the fits to the 42.0- and 52.5-MeV data was achieved by decreasing the

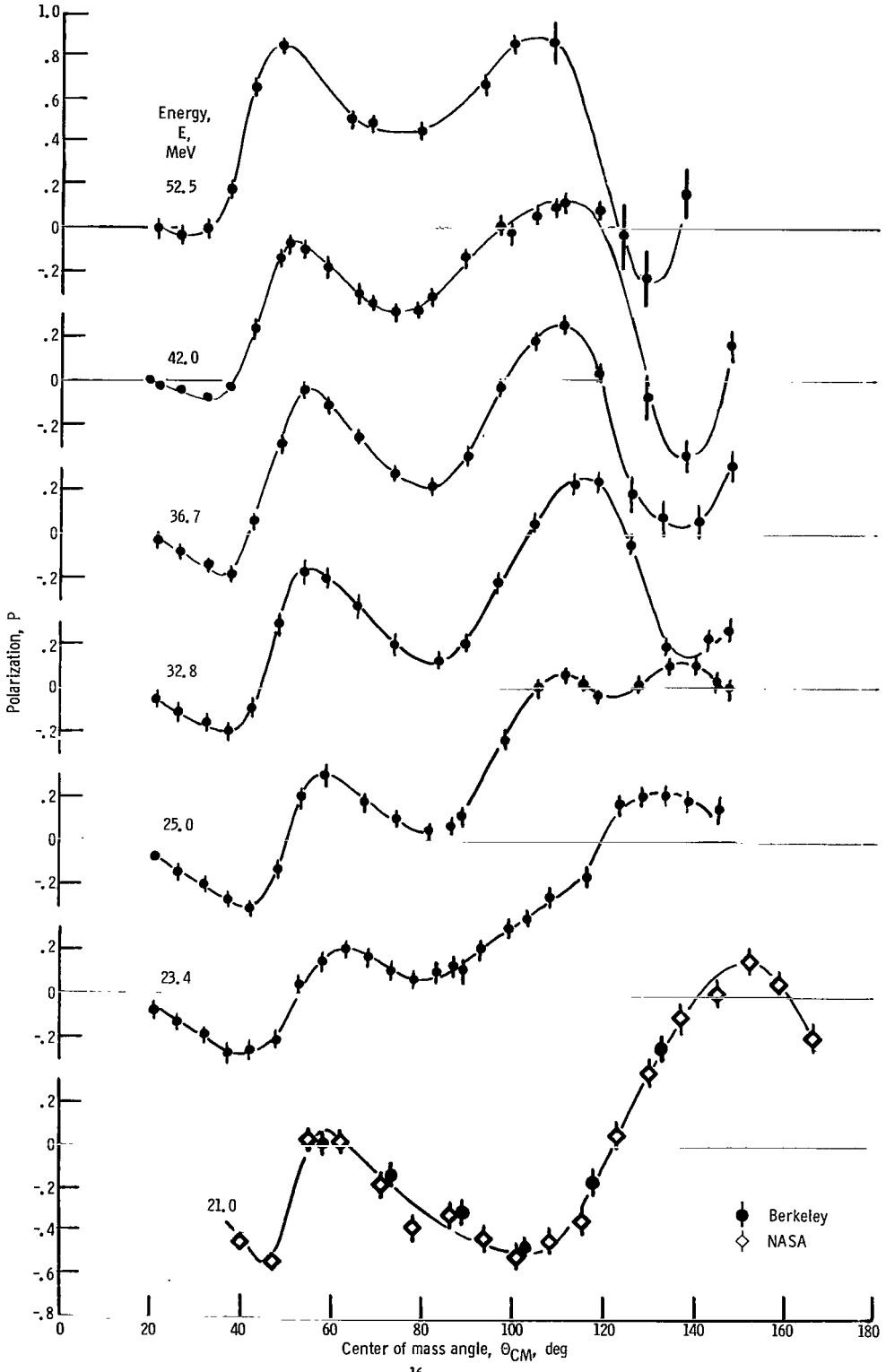

Figure 9. - Energy dependence of polarization p-O^{16} scattering. (Curves are faired through data points. Experimental data taken from refs. 19, 20, and 41).

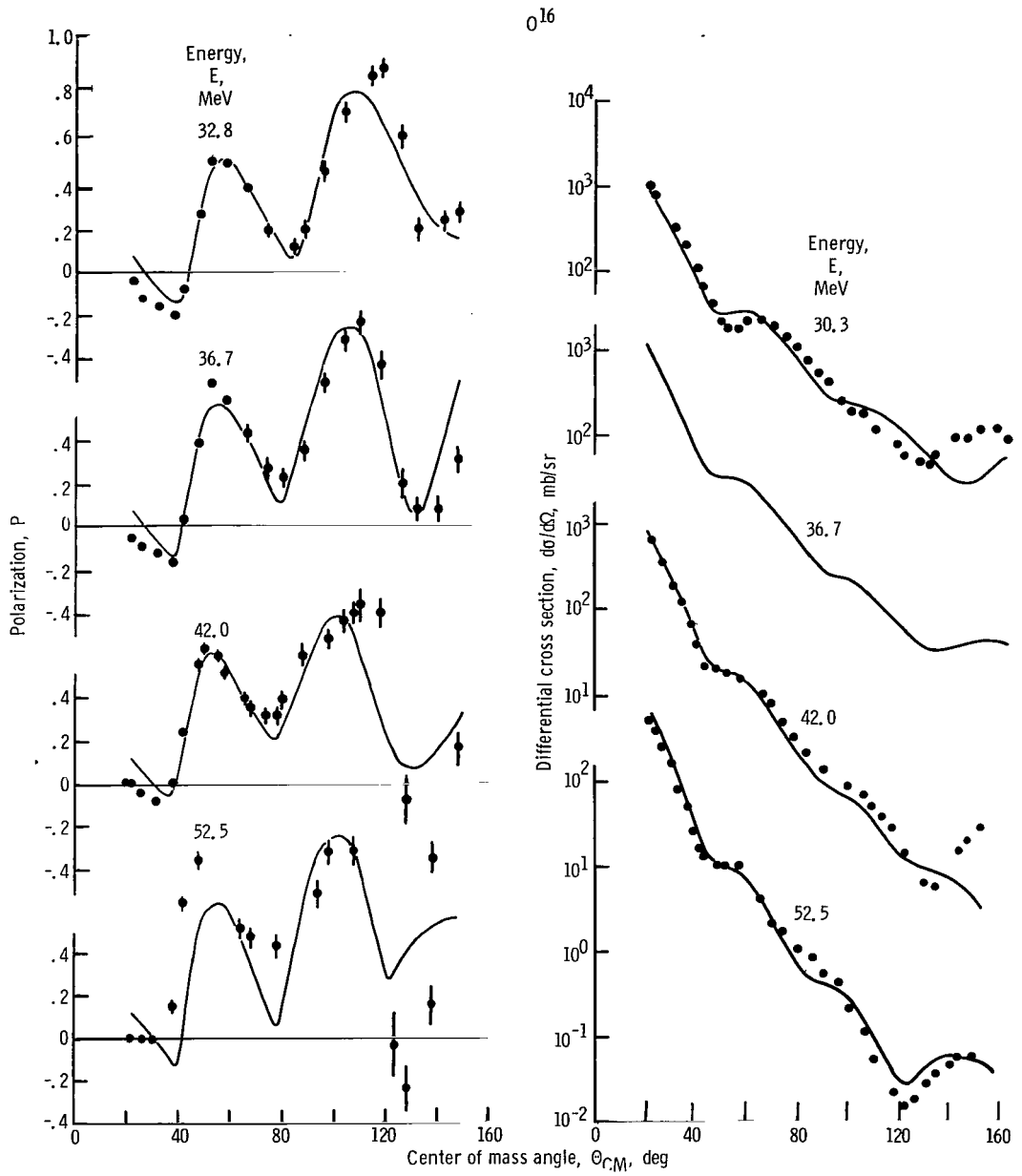

Figure 10. - Comparison of calculated polarizations and differential cross sections for O^{16} (parameters in table IV with experimental data).

TABLE IV. - BEST CONSISTENT PARAMETERS WHEN A SEVEN-PARAMETER POTENTIAL IS USED

Energy, E, MeV	Strength of real potential, V	Strength of surface part of potential, W_D	Strength of spin-orbit potential, V_{so}	Diffuseness of real potential, $a = a_{so}$	Radius of real potential, $r_o = r_{so}$	Width of surface part of potential, a_I	Radius of surface part of potential, r_I
52.5	31.4	3.6	5.7	0.70	1.20	0.44	1.25
42.0	36.0	3.5	8.1	.75	1.20	.76	1.30
36.7	41.3	6.3	8.1	.67	1.25	.50	1.30
32.8	41.0	5.4	7.5	.65	1.25	.50	1.35

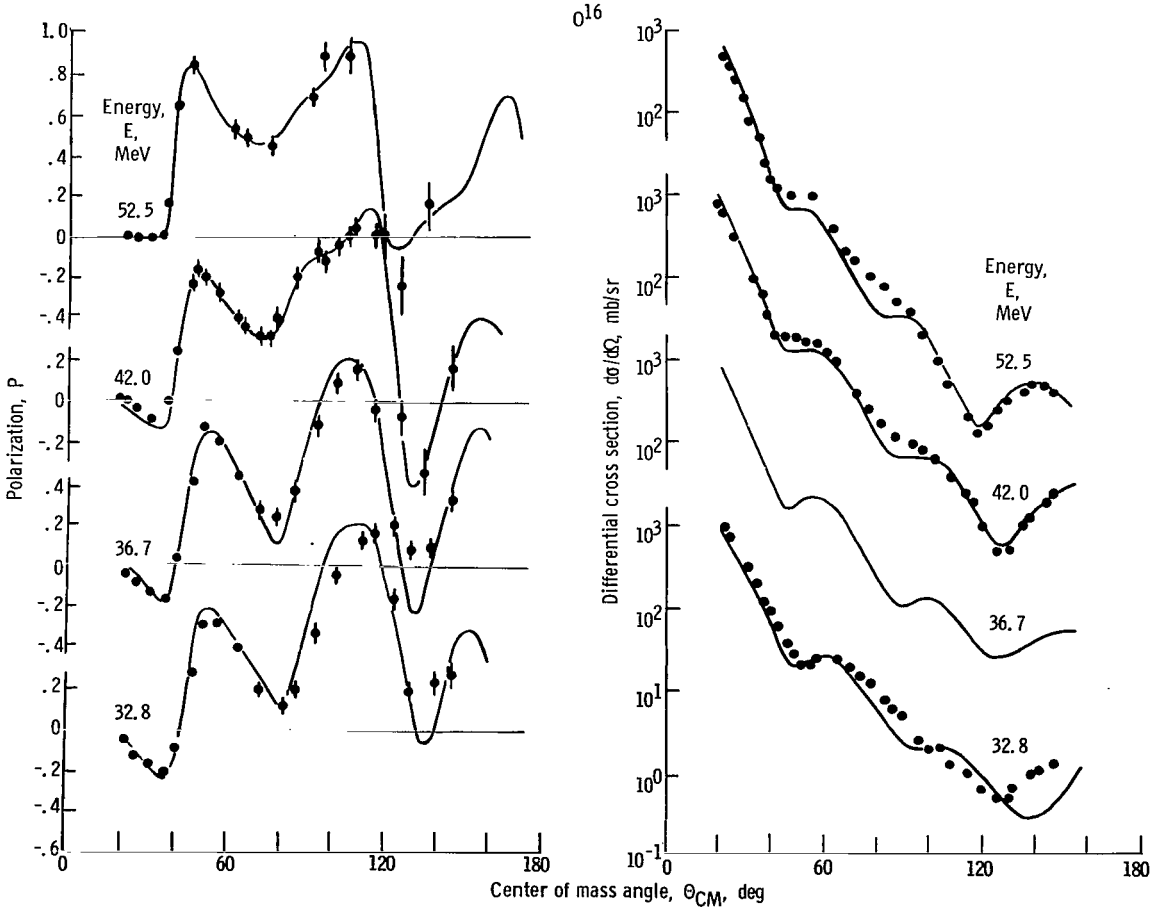

Figure 11. - Best fits obtained to polarizations and differential cross sections for O^{16} with 10-parameter optical potential.

spin-orbit radius. Further improvements were obtained by decreasing a_{so} and adding volume absorption. The best fits obtained are shown in figure 11. By allowing the X^2 values to exceed those of the best fits by a factor of about 2, quite systematic sets of parameters were found (table V).

These paremeters were extrapolated to the lower energies (25.1, 23.4, and 21.1 MeV), but there was no success in fitting the data. An extensive search showed that the parameters which do yield good fits become progressively inconsistent with decreasing energy. The best overall fits to polarizations and cross sections are shown in figure 12, and the corresponding parameters are given in table V. This table shows that in the energy range 30 to 50 MeV five geometrical parameters can be kept constant while the remaining five parameters vary smoothly with energy. The values of V and V_{so} decrease almost linearly with energy. The energy dependence is approximately $dV/dE \approx -1.4$ and $dV_{so}/dE \approx -0.25$.

The total absorption (volume plus surface) stays nearly constant, but the volume absorption increases with proton energy by the same amount as the surface absorption decreases. A puzzling feature is the energy dependence of r_{so}. Many searches show

TABLE V. - BEST CONSISTENT PARAMETERS WHEN A 10-PARAMETER POTENTIAL IS USED

Proton energy, E, MeV	Strength of real potential, V	Strength of surface part of imaginary potential, W_D	Strength of volume part of imaginary potential, W	Strength of spin-orbit potential, V_{so}	Diffuseness of real potential, a	Radius of real potential, r_o	Width of surface part of potential, a_I	Radius of surface part of potential, r_I	Width of spin-orbit potential, a_{so}	Radius of spin-orbit potential, r_{so}
52.5	29.8	3.9	3.0	3.7	0.65	1.25	0.47	1.30	0.47	1.05
42.0	36.1	6.4	1.0	4.4	↓	↓	↓	↓	↓	1.13
36.7	41.1	7.2	---	7.5	↓	↓	↓	↓	↓	1.26
32.8	43.0	7.8	---	8.0	↓	↓	↓	↓	↓	1.22
25.1	39.7	4.7	---	4.3	↓	↓	↓	↓	.38	1.10
23.4	35.6	4.1	---	2.9	↓	↓	↓	↓	.33	1.10
21.0	45.0	10.7	---	2.7	↓	↓	.30	↓	.03	1.08

that it is impossible to obtain satisfactory fits over this energy range with a constant value of r_{so}. At the lower energies the parameters are fairly inconclusive, especially in the case of a_{so}, which becomes unrealistically small at 21.0 MeV.

At the time when this analysis was made, no total reaction cross-section data were available in this energy range. Therefore, only a qualitative comparison could be made between theory and experiment by using total reaction cross-section data (refs. 42, 15, and 43 to 46) for C^{12} and Al^{27} (fig. 13). Recently the total reaction cross section has been measured for p-O^{16} between 27 and 45 MeV (ref. 47). The predictions from this analysis are quite consistent with the data.

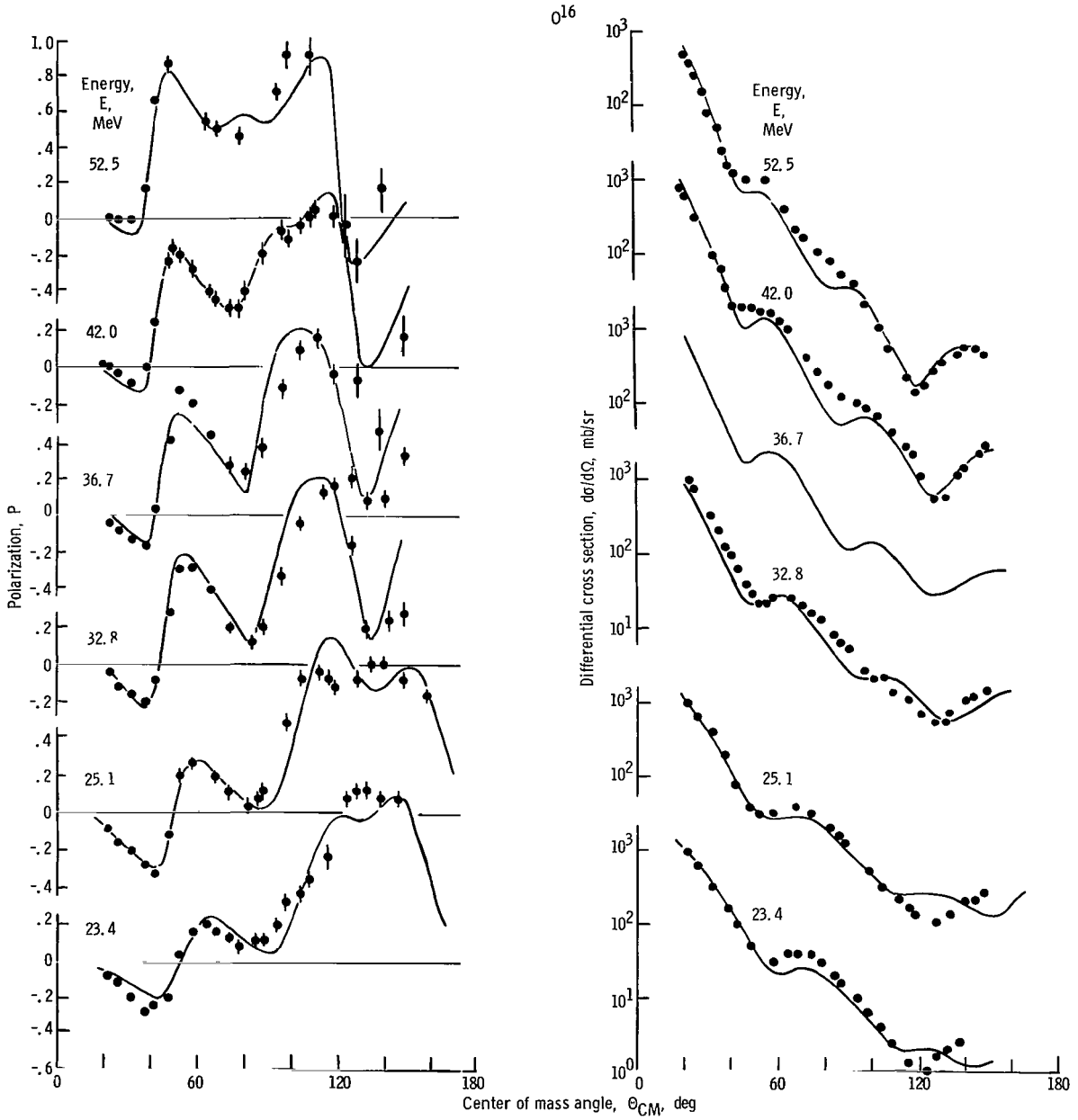

Figure 12. - Best "compromise" fits to polarization and differential cross-section data for O^{16} between 23.4 and 52.5 MeV. As many parameters as possible were kept fixed. Remaining ones were required to follow smooth trends (parameters are listed in table V).

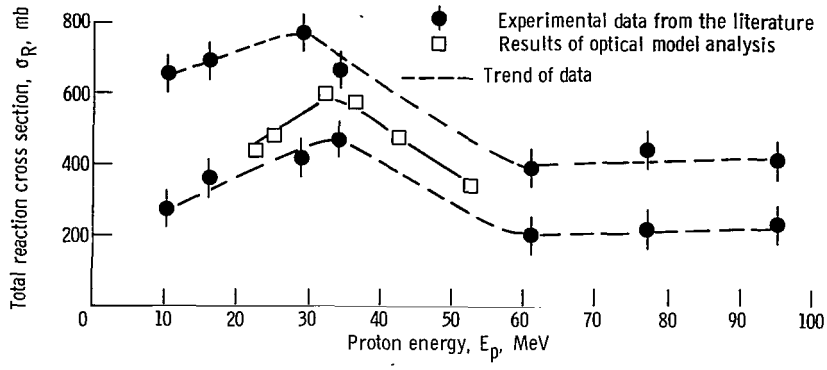

Figure 13. - Total reaction cross sections calculated with parameters in table V shown in comparison with experimental data for C^{12} and Al^{27}.

The proton scattering from O^{16} is presently being studied between 20 and 30 MeV by Appel et al. (ref. 48). When the differential cross sections at large angles were measured as a function of energy, resonances in the elastic scattering channel were observed at incident proton energies of 21.4, 22.3, 23.2, and 27.0 MeV. These resonances may be related to compound states in F^{17}.

COMPARISON WITH OPTICAL MODEL ANALYSES AT HIGHER ENERGIES

For comparison, optical model analyses at higher energies will be briefly described. The discussion is restricted to analyses of polarizations and cross sections for several nuclei, so that average trends in the parameters can be well established. At 30 MeV, differential cross sections, polarizations, and total reaction cross sections have been measured (refs. 7 to 10) for a number of nuclei. Three analyses of these data have been reported.

An optical model study using the differential cross-section data only was made by Barrett et al. (ref. 49) using the geometrical parameters previously determined by Perey in the analysis of 10- to 22-MeV proton scattering data (i.e., $r_o = r_I = r_{so} = 1.25$ F, $a = a_{so} = 0.65$ F, and $a_I = 0.47$ F). Barrett, et al. obtained satisfactory fits to the differential cross sections, except in the backward hemisphere. The polarizations predicted by these parameters, with the use of accepted values for the strength of the spin-orbit potential and the same geometrical parameters as for the real central potential were in qualitative agreement with the experimental data.

A more extensive analysis by Greenlees and Pyle (ref. 50) included polarizations as well as differential cross sections in the multiparameter search. A set of geometrical parameters ($r_o = 1.20$ F, $r_I = 1.25$ F, $r_{so} = 1.10$ F, and $a = a_I = a_{so} = 0.7$ F) was found which gave good fits to both the differential cross section and the polarization data and simultaneously predicted the total reaction cross section correctly. The potential

strengths obtained were consistent with values of other energies. The larger value of the imaginary diffuseness (0.7 F) in comparison with the values from the present analysis (0.65 F) and Perey's work (0.47 F) shows an increase of a_I with energy. This corresponds to the increasing total reaction cross sections. Although Greenlees and Pyle found that good fits were obtained with a predominantly surface form for the imaginary central well, a slight improvement could be achieved by the addition of a small volume part.

The most detailed analysis at this energy was done by Satchler (ref. 34). Satchler observed a smaller radius (r_o = 1.12 F) and a larger diffuseness (a = 0.75 F) for the real central potential than had previously been inferred. The symmetry term (N - Z)/A could be included either in the depth or in the radius of the real well. Satchler also suggested an (N - Z)/A term in the surface absorption potential. A volume absorption of about 3 MeV was required. Fits to the polarizations showed evidence for a spin-orbit coupling with a smaller radius and/or a smaller diffuseness than is used for the real central potential. Satchler proposed two average potentials which gave an equally good overall account of the data. They are given in the following table:

Potential 1	Potential 2
$V = 47.5 + 0.4\frac{Z}{A^{1/3}} + 30\frac{N-Z}{A}$	$V = 51 + 0.4\frac{Z}{A^{1/3}}$
$W_D = 4.5 + 16\frac{N-Z}{A}$	$W_D = 4.25 + 16\frac{N-Z}{A}$
$r_o = 1.12$ F	$r_o = 1.09 + 0.25\frac{N-Z}{A}$
W = 3 MeV; V_{so} = 6.1 MeV; r_I = 1.33 F; r_{so} = 1.0 F; a = a_{so} = 0.75 F;	
$a_I = \begin{cases} 0.58 \text{ F for Fe, Ni, Co, and Cu} \\ 0.65 \text{ F for Sn} \\ 0.75 \text{ F for Pb} \end{cases}$	

Recently, at 40 MeV polarizations and cross sections have been measured (ref. 12) for 11 nuclei between C^{12} and Pb^{208}. The data were analyzed (refs. 12 and 35) in terms of the optical model, and the following "average parameters" were obtained: r_o = 1.16 F, r_I = 1.37 F, r_{so} = 1.06 F, a = 0.75 F, a_I = 0.63 F, a_{so} = 0.74 F, and V_{so} = 6.0 MeV. If the Coulomb correction term is taken to be the same as in Perey's analysis, equal to $0.4\ Z/A^{1/3}$, the real central potential could be described by

$$V = 41.1 + 0.4\frac{Z}{A^{1/3}} + 26.4\frac{N - Z}{A}$$

The depth of the symmetry term in the potential, 26.4 MeV, is in good agreement with Perey's results (ref. 13). Volume, as well as surface absorption, is needed for good fits for nuclei heavier than calcium. The volume absorption varied between ~5 and 7 MeV; the surface absorption increased with nuclear mass from $W_D \approx 1.0$ MeV for Fe^{54} to $W_D \approx 4.5$ MeV for Pb^{208}. The average parameters inferred from this analysis also provide a fairly good fit to the 30-MeV data. By comparing the real well depth at both energies, an energy dependence for the real central well can be obtained; it is $dV/dE = -0.22 \pm 0.03$. This value is less than half of what was found between 10 and 20 MeV.

CONCLUSIONS

An average potential was obtained which is able to predict quite well polarizations, differential cross sections, and total reaction cross sections for a large number of nuclei in the energy range from 16 to 22 MeV. The parameters of this potential are much closer to Perey's parameters than to the ones proposed by Rosen and coworkers. In particular, a dependence on the target mass is clearly established for the real central potential as well as for the depths and width of the surface peaked imaginary potential. For depth, diffuseness, and radius of the spin-orbit potential, the following average parameters were found: $V_{so} = 5.5$ MeV, $a_{so} = 0.55$ F, and $r_{so} = 1.12$ F. The smaller value of r_{so} in comparison with the radius of the real central well $r_o = 1.25$ F is in good agreement with recent results for 30 and 40 MeV. There is no need for an imaginary part or a different form in the spin-orbit potential.

Anomalously low values for the parameters of the spin-orbit potential were encountered in the mass regions of doubly closed shells. No effect of this kind could be clearly established for the closure of only one shell. In the $A = 40$ region the anomaly is energy dependent and is most pronounced at energies where a new partial wave is entering. The large difference in the polarization distribution for Ar^{40} and Ca^{40} near 17 MeV can be ascribed to a difference in the "effective strength," the product of depth and diffuseness of the spin-orbit potential. A smooth energy dependence in this "effective strength" with some of the remaining parameters fixed ($a = a_I = 0.65$ F, $r_o = r_I = 1.25$ F, and $r_{so} = 1.10$ F) and some fluctuating slightly around average values ($V_{Ar} \approx V_{Ca} \approx 47.5$ MeV, $W_{Ar} \approx 7.5$ MeV, $W_{Ca} \approx 5.3$ MeV) can predict the changing polarization and differential cross section for Ar^{40}, K^{39}, and Ca^{40} between 14.5 and 21.0 MeV remarkably well.

The analysis of the energy dependence in p-O^{16} scattering shows that the elastic scattering of protons between 30 and 50 MeV is well described by the optical model. This is in striking contrast to C^{12} where polarization and differential cross-section data have been analyzed in the comparable energy range by Craig and coworkers (29 and 49 MeV) and by Fricke and coworkers (40 MeV). In none of these analyses was it possible to obtain simultaneous fits to polarization and cross-section data. If one tries to extrapolate the optimum parameters for O^{16} between 30 and 50 MeV to lower energies, one meets with increasing difficulties in fitting the data. Fairly good fits can still be obtained at 25.1 and 23.4 MeV with a number of extrapolated parameters, but at 21.0 MeV satisfactory fits can be obtained only with parameters which greatly differ from the extrapolated ones.

Lewis Research Center,
National Aeronautics and Space Administration,
Cleveland, Ohio, October 8, 1968,
129-02-04-06-22.

REFERENCES

1. Rosen, L.; and Brolley, J. E., Jr.: Elastic Scattering of Completely Polarized 10-MeV Protons by Complex Nuclei. Nuclear Physics and Instrumentation. Vol. 14 of the Proceedings of the Second United Nations International Conference on the Peaceful Uses of Atomic Energy. United Nations, 1958, pp. 116-124.

2. Boschitz, E.: Polarization of Protons Elastically and Inelastically Scattered from Carbon Near 17 and 19 MeV. Nucl. Phys., vol. 30, 1962, pp. 468-474.

3. Bercaw, R. W.; Boschitz, E. T.; and Vincent, J. S.: Scattering of 19-MeV Polarized Protons by Light Nuclei. Bull. Am. Phys. Soc., vol. 9, no. 1, 1964, p. 55.

4. Vincent, J. S.: Boschitz, E. T.; and Bercaw, R. W.: Scattering of 19-MeV Polarized Protons by Heavy Nuclei. Bull. Am. Phys. Soc., vol. 9, no. 4, 1964, p. 472.

5. Baugh, D. J.; Greenlees, G. W.; Lilley, J. S.; and Roman, S.: Polarization of 17.8 MeV Protons Scattered by Nuclei. Nucl. Phys., vol. 65, 1965, pp. 33-42.

6. Baugh, D. J.; Griffith, A. R.; and Roman, S.: Polarization of 17.8 MeV Protons Elastically Scattered by Nuclei. Nucl. Phys., vol. 83, 1966, pp. 481-492.

7. Ridley, B. W.; and Turner, J. F.: Optical Model Studies of Proton Scattering at 30 MeV. (I). Differential Cross Sections for Elastic Scattering of Protons at 30.3 MeV. Nucl. Phys., vol. 58, 1964, pp. 497-508.

8. Turner, J. F.; Ridley, B. W.; Cavanagh, P. E.; Gard, G. A.; and Hardacre, A. G.: Optical Model Studies of Proton Scattering at 30 MeV. (II). Proton Total Reaction Cross Sections at 28.5±1.5 MeV. Nucl. Phys., vol. 58, 1964, pp. 509-514.

9. Craig, R. M.; Dore, J. C.; Greenlees, G. W.; Lilley, J. S.; and Lowe, J.: Optical Model Studies of Proton Scattering at 30 MeV. (III). Polarization in Elastic Scattering by Ca, Co^{59}, Ni^{58}, Ni^{60}, Sn^{120}, and Pb^{208}. Nucl. Phys., vol. 58, 1964, pp. 515-521.

10. Calderbank, M.; Burge, E. J.; Lewis, V. E.; and Smith, D. A.: The Elastic and Inelastic Scattering of 50 MeV Protons by ^{64}Zn, ^{66}Zn, ^{68}Zn, and ^{70}Zn. Nucl. Phys., vol. A105, 1967, pp. 601-620.

11. Hwang, C. F.; Clausnitzer, G.; Nordby, D. H.; Suwa, S.; and Williams, J. H.: Polarization of 40-MeV Protons by Complex Nuclei. Phys. Rev., vol. 131, no. 6, Sept. 15, 1963, pp. 2602-2610.

12. Fricke, M. P.; Gross, E. E.; Morton, B. J.; and Zucker, A.: Polarization and Differential Cross Section for Elastic Scattering of 40-MeV Protons. II. Phys. Rev., vol. 156, no. 4, Apr. 20, 1967, pp. 1207-1218.

13. Perey, F. G.: Optical Model Analysis of Proton Elastic Scattering in the Range of 9 to 22 MeV. Phys. Rev., vol. 131, no. 2, July 15, 1963, pp. 745-763.

14. Rosen, Louis; Beery, Jerome G.; and Goldhaber, Alfred S.: Elastic Scattering of 10.5- and 14.5-MeV Polarized Protons from Nuclei and the Optical Model Potential at Intermediate Energies. Ann. Phys. (N.Y.), vol. 34, no. 1, Aug. 1965, pp. 96-152.

15. Pollock, Robert E.; and Schrank, G.: Proton Total Reaction Cross Section at 16.4 MeV. Phys. Rev., vol. 140, no. 3B, Nov. 8, 1965, pp. 575-585.

16. Fulmer, Clyde B.: Total Reaction and Elastic Scattering Cross Sections for 22.8-MeV Protons on Uranium Isotopes. Phys. Rev., vol. 116, no. 2, Oct. 15, 1959, pp. 418-423.

17. Melkanoff, M. A.; Saxon, D. S.; Nodvik, J. S.; and Cantor, D. G.: A FORTRAN Program for Elastic Scattering Analyses with the Nuclear Optical Model. Univ. California Press, 1962.

18. Davidon, William C.: Variable Metric Method for Minimization. Rep. ANL-5990, Argonne National Lab., May 1959.

19. Bercaw, R. W.; Boschitz, E. T.; and Vincent, J. S.: The Scattering of Polarized Protons by Complex Nuclei. Compt. Rend. Congr. Intern. Phys. Nucl., Paris, 1964, vol. 2, pp. 874-876.

20. Bercaw, R. W.; Boschitz, E. T.; and Vincent, J. S.: Elastic Scattering of 21-MeV Polarized Protons by Complex Nuclei. Experientia, Suppl. 12, 1966, pp. 334-335.

21. Dayton, I. E.; and Schrank, G.: Elastic Scattering of 17-MeV Protons by Nuclei. Phys. Rev., vol. 101, no. 4, Feb. 15, 1956, pp. 1358-1367.

22. Eccles, S. F.; Lutz, H. F.; and Madsen, V. A.: Study of the Strongly Excited 2^+ and 3^- States in the $Fe^{54, 56}$ and $Ni^{58, 60, 62}$ Isotopes by Proton Scattering at 18.6 and 19.1 MeV. Phys. Rev., vol. 141, no. 3, Jan. 1966, pp. 1067-1077.

23. Gray, W. S.; Kenefick, R. A.; Kraushaar, J. J.; and Satchler, G. R.: $^{90}Zr(p, p')$ Reaction at 18.8 MeV and the Nuclear-Shell Model. Phys. Rev., vol. 142, no. 3, Feb. 1966, pp. 735-748.

24. Gray, W. S.; Kenefick, R. A.; and Kraushaar, J. J.: Inelastic Proton Scattering. (I). Ar^{40} and Ca^{40}. Nucl. Phys., vol. 67, 1965, pp. 542-564.

25. Gray, W. S.; Kenefick, R. A.; and Kraushaar, J. J.: Inelastic Proton Scattering. (II). Ti^{50} and Fe^{54}. Nucl. Phys., vol. 67, 1965, pp. 565-576.

26. Fulmer, Clyde B.: Elastic Scattering of Protons by Single Isotopes. Phys. Rev., vol. 125, no. 2, Jan. 15, 1962, pp. 631-638.

27. Goldfarb, L. J. B.; Greenlees, G. W.; and Hooper, M. B.: Proton Polarization and the Spin-Orbit Potential. Phys. Rev., vol. 144, no. 3, Apr. 22, 1966, pp. 829-833.

28. Perey, F. G.: Analysis of Elastic Scattering of 17-MeV Protons from Heavy Nuclei. Nuclear Spectroscopy with Direct Reactions. F. E. Throw, ed. Rep. ANL-6848, Argonne National Lab., Mar. 1964, pp. 114-117.

29. Perey, F. G.: Polarization from the Generalized Optical-Potential. Experientia, Suppl. 12, 1966, pp. 191-202.

30. Boschitz, E. T.; Bercaw, R. W.; and Vincent, J. S.: Polarization of 18-MeV Protons Elastically Scattered from the Isobars Ar^{40} and Ca^{40}. Bull. Am. Phys. Soc., vol. 8, no. 8, 1963, p. 611.

31. Volkin, H. C.: Optical-Model Analysis for 18-MeV Protons Elastically Scattered on ^{16}O, ^{40}Ar, ^{39}K, and ^{40}Ca. Bull. Am. Phys. Soc., vol. 9, no. 4, 1964, p. 439.

32. Baugh, D. J.; Dore, J. C.; Greenlees, G. W.; Lowe, J.; and Roman, S.: Polarization of Protons Elastically Scattered by Calcium at 14-18.5 MeV. Phys. Letters, vol. 13, no. 1, Nov. 1, 1964, pp. 63-65.

33. Rosen, L.; and Stewart, L.: Isotopic, and Shell Closure Effects on the Large-Angle Scattering of Polarized Protons. Phys. Rev. Letters, vol. 10, no. 6, Mar. 15, 1963, pp. 246-247.

34. Satchler, G. R.: Optical Model for 30 MeV Proton Scattering. Nucl. Phys., vol. A92, 1967, pp. 273-305.

35. Blumberg, L. N.; Gross, E. E.; van der Woude, A.; Zucker, A.; and Bassel, R. H.: Polarizations and Differential Cross Sections for the Elastic Scattering of 40-MeV Protons from ^{12}C, ^{40}Ca, ^{58}Ni, ^{90}Zr, and ^{208}Pb. Phys. Rev., vol. 147, no. 3, July 22, 1966, pp. 812-825.

36. Nodvik, J. S.; Duke, C. B.; and Melkanoff, M. A.: Optical-Model Analysis of Elastic Scattering of Protons on Carbon at Intermediate Energies. Phys. Rev., vol. 125, no. 3, Feb. 1, 1962, pp. 975-987.

37. Duke, C. B.: Optical-Model Analysis of Elastic Scattering of Protons on Oxygen at Intermediate Energies. Phys. Rev., vol. 129, no. 2, Jan. 15, 1963, pp. 681-691.

38. Baron, Norton; Leonard, Regis F.; and Lind, David A.: Elastic Scattering of 21-MeV Protons from Nitrogen 14, Oxygen 16, Argon 40, Nickel 58, and Tin 116. NASA TN D-4932, 1968.

39. Lowe, J.; and Watson, D. L.: Analysis of Proton-Carbon Elastic Scattering in the Range 20-28 MeV. Phys. Letters, vol. 23, no. 4, Oct. 24, 1966, pp. 261-264. Erratum: Phys. Letters, vol. 24B, no. 4, Feb. 20, 1967, p. 174.

40. Tamura, T.; and Terasawa, T.: Optical Model Plus Resonance Analysis of the Elastic Scattering of Protons by C^{12}. Phys. Letters, vol. 8, no. 1, Jan. 1, 1964, pp. 41-43.

41. Boschitz, E. T.; Chabre, M.; Conzett, H. E.: and Slobodrian, R. J.: Energy Dependence of the Polarization in p-^{16}O Elastic Scattering Between 21 and 53 MeV. Experientia, Suppl. 12, 1966, pp. 331-333.

42. Wilkins, Bruce D.; and Igo, George: 10-MeV Proton Reaction Cross Sections for Several Elements. Phys. Rev., vol. 129, no. 5, Mar. 1, 1963, pp. 2198-2206.

43. Makino, Motoji Q.; Waddell, Charles N.; and Eisberg, Robert M.: Total Reaction Cross Sections for 29 MeV Protons. Nucl. Phys., vol. 50, 1964, pp. 145-156.

44. Gooding, T. J.: Proton Total Reaction Cross Sections at 34 MeV. Nucl. Phys., vol. 12, 1959, pp. 241-248.

45. Meyer, Verena; Eisberg, R. M.; and Carlson, R. F.: Total Reaction Cross Sections of Several Nuclei for 61-MeV Protons. Phys. Rev., vol. 117, no. 5, Mar. 1, 1960, pp. 1334-1336.

46. Goloskie, R.; and Strauch, K.: Measurement of Proton Inelastic Cross Sections Between 77 MeV and 133 MeV. Nucl. Phys., vol. 29, 1962, pp. 474-485.

47. Cameron, J. M.; Carlson, R. F.; Eldridge, H. B.; Richardson, J. Reginald; van Oers, W. T. H.; and Verba, J. W.: Energy Dependence of p-O^{16} Elastic Scattering Between 20 and 50 MeV and the Optical Model. Presented at the International Conference on Nuclear Structure, Tokyo, Sept. 7-13, 1967.

48. Appel, H.; Bunker, S. N.; Cameron, J. M.; Epstein, M. B.; Quinn, J. R.; Richardson, J. Reginald; and Verba, J. W.: Resonances in the Cross Section of Proton Scattering from Oxygen-16 Between 20 and 30 MeV. Bull. Am. Phys. Soc., vol. 13, no. 4, 1968, p. 680.

49. Barrett, R. C.; Hill, A. D.; and Hodgson, P. E.: Optical Model Studies of Proton Scattering at 30 MeV. (IV). Analysis. Nucl. Phys., vol. 62, 1965, pp. 133-144.

50. Greenlees, G. W.; and Pyle, G. J.: Optical-Model Analysis of 30-MeV Proton Scattering. Phys. Rev., vol. 149, no. 3, Sept. 23, 1966, pp. 836-843.

NASA-Langley, 1969 —— 24 E-4583

NATIONAL AERONAUTICS AND SPACE ADMINISTRATION
WASHINGTON, D. C. 20546
OFFICIAL BUSINESS

FIRST CLASS MAIL

POSTAGE AND FEES PAID
NATIONAL AERONAUTICS AND
SPACE ADMINISTRATION

POSTMASTER: If Undeliverable (Section 158 Postal Manual) Do Not Return

"The aeronautical and space activities of the United States shall be conducted so as to contribute . . . to the expansion of human knowledge of phenomena in the atmosphere and space. The Administration shall provide for the widest practicable and appropriate dissemination of information concerning its activities and the results thereof."

— NATIONAL AERONAUTICS AND SPACE ACT OF 1958

NASA SCIENTIFIC AND TECHNICAL PUBLICATIONS

TECHNICAL REPORTS: Scientific and technical information considered important, complete, and a lasting contribution to existing knowledge.

TECHNICAL NOTES: Information less broad in scope but nevertheless of importance as a contribution to existing knowledge.

TECHNICAL MEMORANDUMS: Information receiving limited distribution because of preliminary data, security classification, or other reasons.

CONTRACTOR REPORTS: Scientific and technical information generated under a NASA contract or grant and considered an important contribution to existing knowledge.

TECHNICAL TRANSLATIONS: Information published in a foreign language considered to merit NASA distribution in English.

SPECIAL PUBLICATIONS: Information derived from or of value to NASA activities. Publications include conference proceedings, monographs, data compilations, handbooks, sourcebooks, and special bibliographies.

TECHNOLOGY UTILIZATION PUBLICATIONS: Information on technology used by NASA that may be of particular interest in commercial and other non-aerospace applications. Publications include Tech Briefs, Technology Utilization Reports and Notes, and Technology Surveys.

Details on the availability of these publications may be obtained from:

SCIENTIFIC AND TECHNICAL INFORMATION DIVISION

NATIONAL AERONAUTICS AND SPACE ADMINISTRATION

Washington, D.C. 20546